analytical chemistry

Technical Note

pubs.acs.org/ac

# Functional Packaging of Lateral Flow Strip Allows Simple Delivery of Multiple Reagents for Multistep Assays

Joong Ho Shin and Je-Kyun Park*

Department of Bio and Brain Engineering, Korea Advanced Institute of Science and Technology (KAIST), 291 Daehak-ro, Yuseong-gu, Daejeon 34141, Republic of Korea

Supporting Information

**ABSTRACT:** This paper presents a rotary device designed for facile delivery of multiple reagents to a paper strip for multistep assays. Its purpose is to allow users to easily perform multistep assays and achieve sensitive detection. While the test strip remains stationary, rotating the top piece of the device aligns the reagent and absorbent pads to each end of the paper strip and initiates fluid flow. Further incremental rotation makes an adjacent pair of pads to align simultaneously, causing fluid flow of subsequent reagent that was preloaded in the reagent pad. In this work, various porous substrates were tested to observe their effect on overall flow rate of the system and multistep assays were performed to demonstrate its simple use. As a proof of concept, enzyme-linked immunosorbent assay was carried out to detect *Escherichia coli* O157:H7.

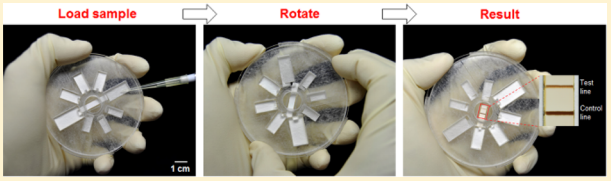


Lateral flow tests (LFT) have been widely used by both professionals and nonprofessionals in a wide range of fields for monitoring purposes[1] because they are portable, economical, rapid, and user-friendly. Despite their advantages, LFTs are still considered to have a high limit of detection.[2] To improve the limit of detection of LFTs, researchers performed multistep assays on LFTs by implementing additional signal amplification steps. Such signal amplification steps utilize either silver or gold enhancer solution to increase the intensity of gold nanoparticle signals. Previous research shows that signal enhancement can lower the detection limit of various targets such as harmful pathogens,[3] toxins,[4] and virus related antigens.[5] The amplification process involves wetting a test strip with enhancer solution after target capture and signal generation steps. However, this step requires additional use of pads and repetitive pipetting, which can limit on-site usage by untrained personnel. Another type of multistep assay on LFT for sensitive detection uses enzyme-linked immunosorbent assay (ELISA). ELISA on LFT has been used for *Escherichia coli* (*E. coli*) O157:H7,[6] *Salmonella typhimurium* (*S. typhimurium*),[7] and hepatitis B surface antigen detections.[8] The strip-based ELISA requires a capture and labeling step of target analyte, and then a signal generation step. However, because an absorbent pad cannot absorb more fluid after its full capacity, this process requires manual replacement of a wetted absorbent pad with a new absorbent pad, along with the use of a new sample pad for signal generation step. This requirement for the replacement or rearrangement of pads can be difficult for untrained personnel and can also expose users to potentially harmful samples. Thus, for practical application by a wide range of users, a robust and functional packaging system that can perform sequential delivery of multiple reagents to a paper strip in a simple manner is required.

There are few studies that show advances in the LFT packaging technologies. For example, cross-flow chromatography, which consists of first flow along the length of the strip and a second flow across the width of the strip, was made simple by using a plastic chip.[9,10] Although the chip allowed simple handling, it was limited in the number of reagents that can be used. For practical applications, an integrated paper-based fluidics technology with a foldable plastic packaging was developed to perform automated three-step assay that includes sample-gold nanoparticle conjugation, washing, and signal amplification steps.[11,12] The device has three paper channels of different path lengths and utilizes channel resistance and delayed arrival of fluids to sequentially deliver multiple reagents to a test zone. With the advance in paper-based fluidics, controllable fluid delay technologies with the same goal have been developed. Such technologies achieved delayed fluid flow by treating the paper channels with different concentrations of sugar,[13] laser-induced photopolymerization,[14] or by pressing nonwoven polypropylene-based paper channel to create channel resistance.[15] However, multistep assay platforms that utilize channel resistance for fluid delays are subject to inevitably increased assay duration, which can last up to 40 min[11,15] to an hour to complete the assay.[12] This is because channel resistances of subsequent reagents' channels have to be increased in order to delay the arrival time of the reagents, which ends up decreasing its flow rate and thereby increasing the total time required to process the subsequent reagents. It is an inherent limitation of the delay-based systems, whose assay duration inevitably increases with increased number of

**Received:** July 26, 2016
**Accepted:** October 5, 2016
**Published:** October 5, 2016





DOI: 10.1021/acs.analchem.6b02869
*Anal. Chem.* 2016, 88, 10374−10378

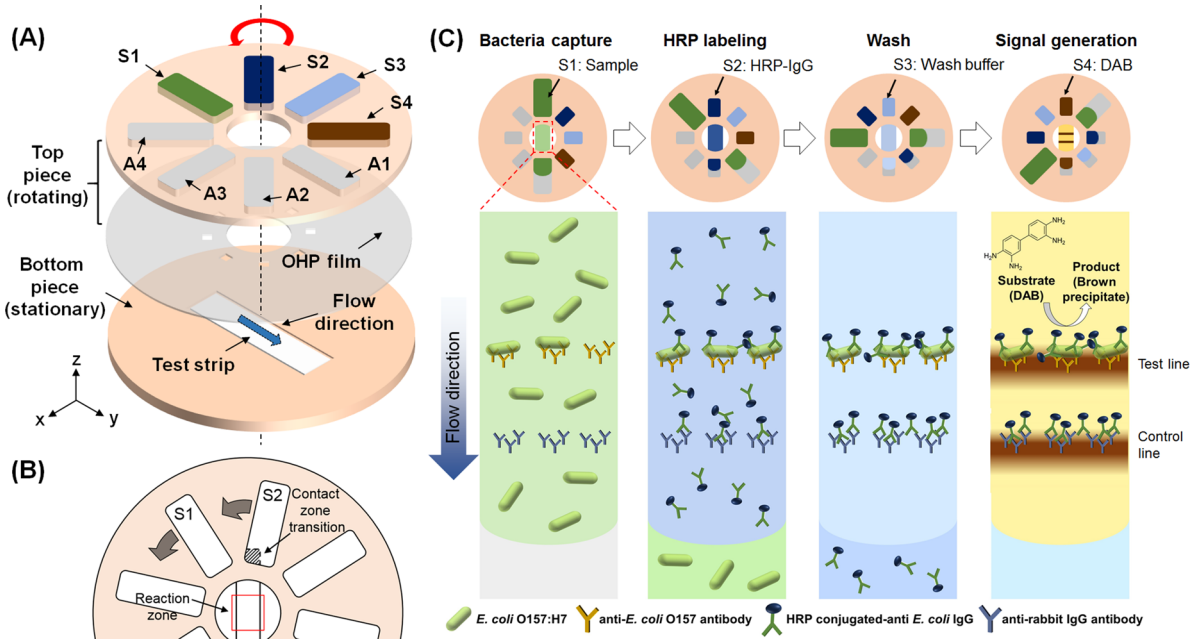


**Figure 1.** Principle of a rotary device for simple delivery of multiple reagents and multistep assays. (A) Exploded view of the rotary device showing its components and its layers. (B) Schematic of the top view showing the transition of contact zone during rotation. (C) Schematics of each step of strip-based ELISA showing bacteria capture, HRP-IgG labeling, wash, and signal generation steps.

additional fluidic channels and assay steps. Thus, a new platform that can versatilely deliver multiple reagents without deterred flow rate is needed.

In this study, we introduce a packaging method for simple sequential delivery of multiple reagents to a test strip. It consists of two portions that can rotate with respect to each other, and incremental rotation of the device facilitates simultaneous rearrangement of sample and absorbent pads, thereby facilitating sequential delivery of multiple reagents. The packaging allows simple execution of multistep assays by rotating the device by hand. As a proof of concept, we perform ELISA on a lateral flow strip and demonstrate simple colorimetric detection of *E. coli* O157:H7.

## EXPERIMENTAL SECTION

**Design and Fabrication.** The device is designed to simplify the complicated and laborious multistep assays. It consists of a stationary part (bottom piece) and a rotating part (top piece) (Figure 1A). Sample pads (S1−S4) and their corresponding absorbent pads (A1−A4) are contained in the top piece and nitrocellulose (NC) test strip is contained in the bottom piece. A patterned OHP transparency film, which has through-holes, is attached to the bottom of the top piece. This enables direct contact between the sample pad and test strip and also between the test strip and absorbent pad. The top and bottom pieces were made from 3 mm-thick poly(methyl methacrylate) (PMMA) plates, which were patterned and etched by a laser cutter (C40-60W; Coryart, Anyang, Korea). The diameter of the hand-held device was 8 cm. The through-holes were patterned on the OHP film by a laser cutter and then adhered to the top piece with double-sided tape.

**Device Operation.** The top piece of the device can be oriented so that each end of the test strip can contact the sample pad and absorbent pad. Reagent is loaded into the sample pad, flows through the NC strip, and then absorbed by the absorbent pad. As shown in Figure 1B, rotating the top piece counterclockwise about the *z*-axis disconnects both the sample pad (S1) and the absorbent pad (A1) from the test strip; and the subsequent sample pad (S2), along with a new absorbent pad (A2) connects with each end of the strip. All reagents can be loaded to the sample pads in the beginning of an assay. This process can be further simplified by storing the reagents in a dried form and rehydrating them prior to the experiment.[12,16] Then, the reagents can be sequentially delivered to the test strip simply by incrementally rotating the top piece of the device with hands. In this study, capture antibodies were immobilized at the reaction zone of the test strip.

**Flow Rate Evaluation.** Materials for sample pad and pore size for NC membrane were selected based on their capillarity and permeability. A glass fiber pad (GFDX103000; Millipore, Billerica, MA) and a cellulose pad (Grade 319; Ahlstrom, Finland) were chosen as materials for sample pad and compared based on their pore size. The pore sizes of each pad were measured by mercury intrusion porosimetry (Autopore IV9500; Micrometrics Instrument Corporation, GA). NC membranes of three different pore sizes (CNPF-SN12, 8 $\mu$m; CNPF-SN12 10 $\mu$m; CNPC-SS12, 15 $\mu$m) were purchased from Advanced Microdevices (India), and the absorbent pad was purchased from Ahlstrom (grade 222). To observe the effect of sample pad's backpressure on flow rate, NC membrane (15 $\mu$m pore size) was cut into 4 mm × 25 mm strips. Each end of the strips was overlapped with a sample pad and an absorbent pad, respectively. A volume of 100 $\mu$L of blue dye was dropped onto the sample pad and the absorption rate was measured by measuring the wetted area of the absorbent pad every 2 min. To observe the effect of NC membrane's pore size on flow rate, the same experiment was performed using NC strips of different pore sizes while using a glass fiber pad as a sample pad.

**Enzyme-Linked Immunosorbent Assay (ELISA) on a Lateral Flow Strip.** As a demonstration of facile execution of multistep assay, ELISA was performed for *E. coli* O157:H7



DOI: 10.1021/acs.analchem.6b02869
*Anal. Chem.* 2016, 88, 10374−10378

(ATCC 35150) detection. Anti-*E. coli* O157 antibody (ab20976; Abcam) was dispensed as a test line and antirabbit IgG (A120-100A; Bethyl, Montgomery, TX) was dispensed (3.5 mm away from the test line) as a control line (both were diluted to 1 mg/mL) on 15 $\mu$m pore size NC membrane. The sizes of sample pads were adjusted to contain 90 $\mu$L of sample (S1), and 40 $\mu$L of assay reagents (S2−S4) and the size of their respective absorbent pads were also adjusted accordingly.

As shown in Figure 1C, the detection process involves bacteria capture, labeling, wash, and signal generation steps in the specific order. First, 40 $\mu$L of horseradish peroxidase (HRP)-conjugated anti-*E. coli* IgG (ab20425; Abcam) (10 ng/mL) in a phosphate buffered saline (PBS) containing 3% bovine serum albumin (BSA) and 0.05% Tween-20 was loaded into S2. Next, 40 $\mu$L of PBS containing 3% BSA and 0.05% Tween-20 was loaded into S3 to be used as a wash buffer. Then, 40 $\mu$L of 3,3′-diaminobenzidine (DAB) (Sigma-Aldrich) solution, which was prepared by dissolving and mixing two tablets in 15 mL of deionized water, was loaded into S4. Pads S2−S4 were saturated just prior to loading the sample. To begin the assay, 90 $\mu$L of *E. coli* O157:H7 suspended in 2% BSA was loaded into S1 for bacteria capture step, during which bacteria flows through the porous network of NC strip and were captured by the capture antibodies. Although preliminary experimental result suggests that evaporation over the course of entire assay does not have detrimental effect on the result (data not shown), an OHP film was placed on top of the device after loading reagents and samples to minimize any effect of variation in humidity and also to keep the experimental condition consistent. After bacteria capture step, the top piece was rotated 45° counterclockwise to deliver HRP-conjugated IgG for 5 min. The HRP-conjugated IgGs bind with the captured bacteria and unbound HRP-conjugated IgGs that flow past the test line bind with antirabbit IgGs at the control line. Then the top piece was further rotated to align S3 with the strip for the 3 min wash step. This washes HRP-conjugated IgGs that are nonspecifically present throughout the NC strip. Lastly, S4 was aligned with the strip with further rotation, and DAB was converted into brown precipitates by HRP for 4 min. Formation of brown precipitates at the test line indicates the presence of target analyte, and the formation of control line indicates that the assay has been performed properly.

To investigate the effect of sample flow duration and DAB flow duration on the intensity of signal, bacteria ($5 \times 10^5$ CFU/mL) was allowed to flow for 5, 10, 15, and 20 min and their respective detection signals were imaged after 2 and 4 min of DAB flow. To determine the limit of detection, *E. coli* O157:H7 was serially diluted (log-dilution in each step) in concentrations ranging from $5 \times 0$ to $10^8$ CFU/mL, and their detection signals were quantified using ImageJ software (NIH).

## RESULTS AND DISCUSSION

**Sample Pad Backpressure and Strip Resistance.** The flow phenomena in the device can be divided into two stages: strip wetting flow and absorbent pad wetting flow. First, reagent in the sample pad wicks through and wets the NC strip by capillary action (Figure 2A). Then the reagent in sample pad flows through the wetted NC strip and to absorbent pad (Figure 2B). The flow rate is determined by the properties of each material: the pore size of NC membrane and the difference in capillary pressure between the absorbent pad and sample pad. The materials that allows higher flow rate were selected in order to process more volume per unit time. By

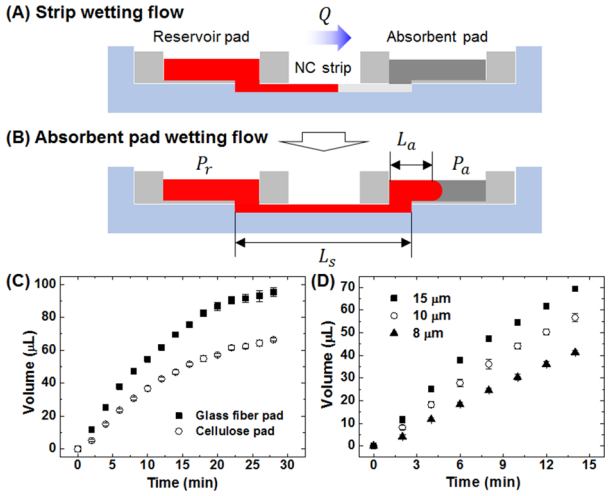


**Figure 2.** Effect of sample pad's backpressure and strip resistance. Schematic of cross sections of red reagent flowing (A) during strip wetting flow and (B) absorbent pad wetting flow. (C) Graph showing the effect of back pressure exerted by glass fiber and cellulose pad. (D) Graph showing the effect of strip's pore size on flow rate.

modifying the reduced form of Darcy's law,[17] and adding resistances of materials in series,[18] flow rate during absorbent pad wetting flow can be described by following equation:

$$Q = \frac{P_a - P_r(t)}{\mu\left(\frac{L_s}{\kappa_s W_s H_s} + \frac{L_a(t)}{\kappa_a W_a H_a}\right)}$$

where $Q$ is the flow rate, $P_a$ is capillary pressure of absorbent pad, $P_r(t)$ is capillary pressure of sample pad, $\mu$ is viscosity of liquid, $L_s$ is the length of NC strip, $\kappa_s$ is permeability of the strip, $W_s$ is the width of the strip, $H_s$ is the thickness of the strip, $L_a(t)$ is the length of the wetted area of absorbent pad, $K_a$ is the permeability of the absorbent pad, $W_a$ is the width of the absorbent pad, and $H_a$ is the thickness of the absorbent pad. The wetted NC strip can be considered as a resistor ($\mu L_s/\kappa_s W_s H_s$) and the wetted portion of the absorbent pad can be considered as a variable resistor ($\mu L_a(t)/\kappa_a W_a H_a$) whose viscous resistance increases over time. According to the equation, the flow rate is driven by the difference between the capillary pressure of the absorbent pad and the sample pad. During the absorbent pad wetting flow, $P_a$ drives the fluid flow whereas $P_r(t)$ opposes the flow by exerting back pressure. The back pressure exists because the porous materials used as a sample pad are nonideal fluid sources, which are reported to cause back pressure that increases over time as the sample pad drains.[19]

We first compared the difference in back pressure exerted by different materials. We chose a cellulose pad and a glass fiber pad because they both are widely used materials of lateral flow assay devices. The porous space of sample pad can be modeled as a bundle of parallel capillaries and its capillary pressure can be described by the Young−Laplace equation: $P = 2\gamma \cos\theta/r$, where $\gamma$ is the air−liquid surface tension, $\theta$ is the contact angle of liquid−solid, and $r$ is the effective radius of the porous space. According to the equation, the sample pad with smaller pore size results in higher capillary pressure, which means it is more likely to hold on to the liquid and prevent it from flowing toward the absorbent pad. The mean pore size of the glass fiber pad and cellulose pad was measured to be 105.60 and 5.71 $\mu$m, respectively. This means that the cellulose pad theoretically


DOI: 10.1021/acs.analchem.6b02869
Anal. Chem. 2016, 88, 10374−10378

exerts greater back pressure compared to glass fiber pad due to its smaller pore size. Scanning electron microscopic images also show that the fibers are more closely packed together with less empty space (Figure S1 of the Supporting Information). As shown in Figure 2C, when the cellulose pad was used as a sample pad, the resulting flow rate is lower compared to using the glass fiber pad. This difference in flow rate is largely due to the difference in the average pore size of the pads. Thus, we chose glass fiber over cellulose pad because it exerts less back pressure and allows its reagents to be drained at higher flow rates.

The flow rate equation also shows that the flow rate increases as the permeability of the NC strip increases. The permeability of the NC strips are proportional to their pore sizes (specified by manufacturer), thus we compared the strips based on their pore size. Figure 2D shows that larger pore size allows higher flow rate as expected. Larger pore size means larger permeability, which reduces viscous resistance in the NC strip and results in higher flow rate. On the basis of these results, a glass fiber pad and 15 $\mu$m pore size NC strip were chosen to decrease the time required to process the sample and assay reagents.

**Hand-Operated ELISA for Foodborne Pathogen Detection.** The intensity of detection signal can be affected by the number of captured bacteria, which is largely affected by the duration of the sample flow. Thus, the effect of sample flow duration on the signal intensity was investigated. With increased duration of sample flow, more bacteria can be captured by the capture antibodies, and stronger signal can be generated. It is clear that the detection signal becomes stronger if the sample was allowed to flow for longer time, and longer DAB flow also results in stronger signal as well (Figure 3). The

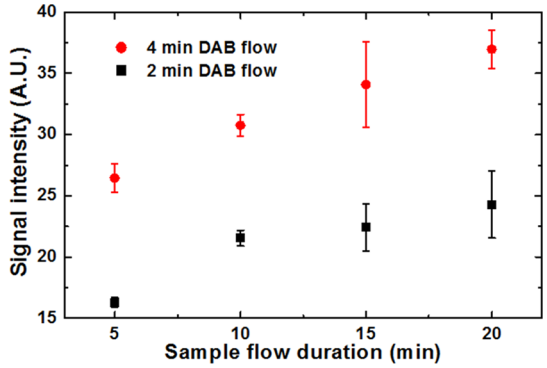


**Figure 3.** Effects of sample and DAB flow duration. Graph shows the signal intensities with varying sample flow duration and DAB flow duration.

trend in Figure 3 suggests that signal intensity may increase with longer sample flow duration. However, increasing the duration can also increase the total time required to complete the assay and may not be suitable for rapid analysis. Thus, we limited the sample flow to 20 min and compared detection limit of 10 and 20 min sample flow, which requires a total assay time of 22 and 32 min, respectively.

Figure 4A,B shows the detection results of *E. coli* O157:H7 of varying concentrations after 20 and 10 min sample flow with 5 min HRP labeling, 3 min wash, and 4 min DAB flow. The assay results of both 10 and 20 min sample flow show distinguishable signal from the test line (TL) starting $5 \times 10^4$ CFU/mL of *E. coli* O157:H7 and the intensity increases with increasing

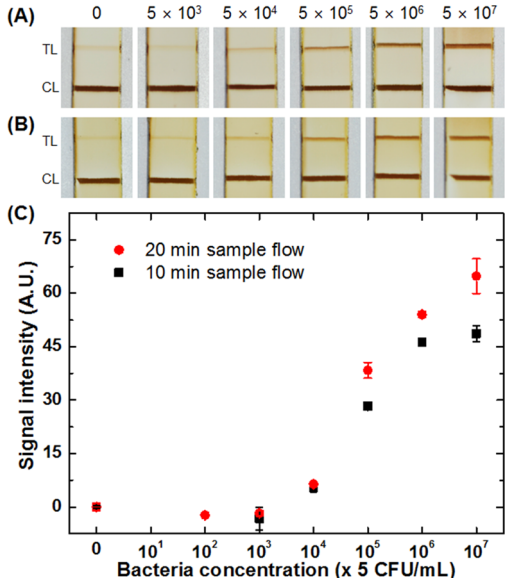


**Figure 4.** *E. coli* O157:H7 detection results. Photos of varying concentrations of *E. coli* O157:H7 detection result with (A) 20 min and (B) 10 min sample flow duration. (C) Graph showing the intensities of 20 and 10 min sample flow assay results with respect to bacteria concentration.

concentration of the bacteria. Figure 4C shows that 20 min sample flow results in stronger signal intensity compared to 10 min sample flow; however, their limit of detection is the same ($5 \times 10^4$ CFU/mL). It is worth noting that 10 min sample flow can offer just as sensitive assay result as 20 min sample flow, and that the assay can be finished in a total of 22 min. This is largely due to the fact that antibody−antigen binding is a reversible process that involves constant binding and separation, which means that increasing the sample flow duration beyond the time required to reach equilibrium is not necessary nor does it improve the limit of detection. Using antibodies with higher affinity is one of promising ways to lower the detection limit.

On the basis of these results, it is clear that the device helps perform multistep assays with ease by allowing users to control not only the sequence but also the duration of fluid delivery. The device can be particularly useful for performing assays that require specific number of steps with specific set of sequences for proper operation (Figure S2 of the Supporting Information). Furthermore, the ability to report consistent signal intensities regardless of the variation in loading sample volume (Figure S3 of the Supporting Information) can be a useful feature for on-site monitoring purposes, where users may load imprecise volume of samples with tools such as disposable transfer pipets. Although the current format requires loading of several reagents before the experiment, this process can be further simplified by storing them in blister packs and bursting them open prior to use.[20,21] Such integration is expected to further simplify the assay and make it more suitable for on-site applications by a wide range of users.

## CONCLUSION

In this proof of concept study, we demonstrated a hand-held device that can easily perform multistep assays on a LFT strip. The device allows users to control the order and duration of fluid delivery, thereby simplifying the delivery process of multiple reagents on the strip. Different materials of sample


DOI: 10.1021/acs.analchem.6b02869
*Anal. Chem.* 2016, 88, 10374−10378

pads and NC strips of varying pore sizes were tested, and materials that allow larger volumetric flow rate were chosen to minimize sample processing time. The device was then used to demonstrate simple operation of strip-based ELISA for *E. coli* O157:H7 detection.

The main novelty of the device is that it allows users to perform multiple assay steps through a simple and familiar hand motion similar to, for example, opening a jar. Unlike the previous methods that require manual rearrangement of pads,[7,22] the proposed design allows simultaneous rearrangement of both sample pad and absorbent pad with each incremental rotation.

The device is not limited to four-step assay as demonstrated. Its design can be expanded to process more number of reagents and can be utilized to perform more complicated multistep procedures such as large volume sample pretreatment[23] and paper-based polymerase chain reaction.[24] We expect this device to be used by untrained personnel as well as trained professionals for a wide range of purposes, including point of care diagnosis, environmental monitoring, and on-site detection.

## ■ ASSOCIATED CONTENT

### Supporting Information

The Supporting Information is available free of charge on the ACS Publications website at DOI: 10.1021/acs.analchem.6b02869.

SEM images of cellulose pad and glass fiber pad (Figure S1), assay sequence optimization (Figure S2), and loading volume effect (Figure S3) (PDF)

## ■ AUTHOR INFORMATION


### Corresponding Author

*E-mail: jekyun@kaist.ac.kr. Phone: +82-42-350-4315. Fax: +82-42-350-4310.


### Notes

The authors declare no competing financial interest.

## ■ ACKNOWLEDGMENTS

This research was supported by a Cooperative Research Program for Agricultural Science and Technology Development (Grant No. PJ009842) supported by the Rural Development Administration of Korea, by a Mid-Career Researcher Program (Grant No. NRF-2016R1A2B3015986), and a Bio & Medical Technology Development Program (Grant No. NRF-2015M3A9B3028685) through the National Research Foundation of Korea funded by the Ministry of Science, ICT and Future Planning. The authors also acknowledge Dr. Seyong Kwon for helpful discussions.

## ■ REFERENCES


(1) Posthuma-Trumpie, G. A.; Korf, J.; van Amerongen, A. *Anal. Bioanal. Chem.* **2009**, *393*, 569−582.

(2) Choi, S.; Lee, J.-H.; Kwak, B. S.; Kim, Y. W.; Lee, J. S.; Choi, J.-S.; Jung, H. I. *BioChip J.* **2015**, *9*, 116−123.

(3) Anfossi, L.; Di Nardo, F.; Giovannoli, C.; Passini, C.; Baggiani, C. *Anal. Bioanal. Chem.* **2013**, *405*, 9859−9867.

(4) Yang, W.; Li, X.-B.; Liu, G.-W.; Zhang, B.-B.; Zhang, Y.; Kong, T.; Tang, J.-J.; Li, D.-N.; Wang, Z. *Biosens. Bioelectron.* **2011**, *26*, 3710−3713.

(5) Wada, A.; Sakoda, Y.; Oyamada, T.; Kida, H. *J. Virol. Methods* **2011**, *178*, 82−86.

(6) Park, S.; Kim, H.; Paek, S.-H.; Hong, J. W.; Kim, Y.-K. *Ultramicroscopy* **2008**, *108*, 1348−1351.

(7) Park, S.; Kim, Y. T.; Kim, Y.-K. *BioChip J.* **2010**, *4*, 110−116.

(8) Cho, J.-H.; Paek, E.-H.; Cho, I.-H.; Paek, S.-H. *Anal. Chem.* **2005**, *77*, 4091−4097.

(9) Cho, I.-H.; Seo, S.-M.; Paek, E.-H.; Paek, S.-H. *J. Chromatogr. B: Anal. Technol. Biomed. Life Sci.* **2010**, *878*, 271−277.

(10) Cho, J.-H.; Han, S.-M.; Paek, E.-H.; Cho, I.-H.; Paek, S.-H. *Anal. Chem.* **2006**, *78*, 793−800.

(11) Fu, E.; Liang, T.; Spicar-Mihalic, P.; Houghtaling, J.; Ramachandran, S.; Yager, P. *Anal. Chem.* **2012**, *84*, 4574−4579.

(12) Fridley, G. E.; Le, H.; Yager, P. *Anal. Chem.* **2014**, *86*, 6447−6453.

(13) Lutz, B.; Liang, T.; Fu, E.; Ramachandran, S.; Kauffman, P.; Yager, P. *Lab Chip* **2013**, *13*, 2840−2847.

(14) He, P. J. W.; Katis, I. N.; Eason, R. W.; Sones, C. L. *Lab Chip* **2015**, *15*, 4054−4061.

(15) Shin, J. H.; Park, J.; Kim, S. H.; Park, J.-K. *Biomicrofluidics* **2014**, *8*, 054121.

(16) Ramachandran, S.; Fu, E.; Lutz, B.; Yager, P. *Analyst* **2014**, *139*, 1456−1462.

(17) Osborn, J. L.; Lutz, B.; Fu, E.; Kauffman, P.; Stevens, D. Y.; Yager, P. *Lab Chip* **2010**, *10*, 2659−2665.

(18) Park, J.; Shin, J. H.; Park, J.-K. *Micromachines* **2016**, *7*, 48.

(19) Dharmaraja, S.; Lafleur, L.; Byrnes, S.; Kauffman, P.; Buser, J.; Toley, B.; Fu, E.; Yager, P.; Lutz, B. Programming paper networks for point of care diagnostics. In *SPIE MOEMS-MEMS*, San Francisco, CA, February 2, 2013; 86150X, 10.1117/12.2006138.

(20) Smith, S.; Naidoo, T.; Davies, E.; Fourie, L.; Nxumalo, Z.; Swart, H.; Marais, P.; Land, K.; Roux, P. Sample to answer visualization pipeline for low-cost point-of-care blood cell counting. In *SPIE BIOS*, San Francisco, CA, February 7, 2015; 93320V, 10.1117/12.2076751.

(21) Becker, H.; Hlawatsch, N.; Haraldsson, T.; van der Wijngaart, W.; Lind, A.; Malhotra-Kumar, S.; Turlej-Rogacka, A.; Goossens, H. Microfluidic system for the identification of bacterial pathogens causing urinary tract infections. In *SPIE BiOS*, San Francisco, CA, February 7, 2015; 93200S, 10.1117/12.2077644.

(22) Wang, J.-Y.; Chen, M.-H.; Sheng, Z.-C.; Liu, D.-F.; Wu, S.-S.; Lai, W.-H. *RSC Adv.* **2015**, *5*, 62300−62305.

(23) Byrnes, S.; Bishop, J.; Lafleur, L.; Buser, J.; Lutz, B.; Yager, P. *Lab Chip* **2015**, *15*, 2647−2659.

(24) Connelly, J. T.; Rolland, J. P.; Whitesides, G. M. *Anal. Chem.* **2015**, *87*, 7595−7601.




DOI: 10.1021/acs.analchem.6b02869
*Anal. Chem.* 2016, 88, 10374−10378